

# Joint Link Adaptation and User Scheduling With HARQ in Multicell Environments

Su Min Kim, *Member, IEEE*, Bang Chul Jung, *Senior Member, IEEE*, and Dan Keun Sung, *Fellow, IEEE*

**Abstract**—Intercell interference (ICI) is one of the most critical factors affecting performance of cellular networks. In this paper, we investigate a joint link adaptation and user scheduling problem for a multicell downlink employing hybrid automatic repeat request (HARQ) techniques, where the ICI exists among cells. We first propose an approximation method on aggregated ICI for analyzing an effective signal-to-interference-and-noise ratio (SINR) with the HARQ technique at users, which is known as identical path-loss approximation (IPLA). Based on the proposed IPLA, we propose a transmission rate selection algorithm maximizing an expected throughput at each user. We also propose a simple but effective cross-layer framework jointly combining transmission rate adaptation and user scheduling techniques, considering both HARQ and ICI. It is shown that the statistical distribution of the effective SINR at users based on the IPLA agrees well with the empirical distribution, while the conventional Gaussian approximation (GA) does not work well in the case that dominant ICIs exist. Thus, IPLA enables base stations (BSs) to choose more accurate transmission rates. Furthermore, the proposed IPLA-based cross-layer policy outperforms existing policies in terms of both system throughput and user fairness.

**Index Terms**—Cross-layer optimization, hybrid automatic repeat request (HARQ), intercell interference (ICI), link adaptation, user scheduling.

## I. INTRODUCTION

COMPENSATION for uncertain fading phenomena is one of the most challenging issues in wireless communications. To improve link reliability and radio resource efficiency against such uncertainty, a *hybrid automatic repeat request* (HARQ) technique has been proposed in the physical (PHY) layer [1]–[3]. Meanwhile, in the medium access control (MAC) layer, *dynamic link adaptation* [4], [5] and *user scheduling* [6], [7] techniques have been exploited by using channel-state information (CSI) at the transmitter for point-to-point

and multiuser (MU) environments, respectively. There have existed many studies on link adaptation considering HARQ for various fading channel models in point-to-point communications [8]–[12]. Moreover, several user scheduling algorithms considering HARQ have been proposed for MU environments in single-cell networks [13]–[17]. Through these studies considering HARQ techniques, the resource efficiency of wireless communications has been improved.

By the way, intercell interference (ICI) is another key factor to determine overall system performances in multicell networks. In traditional code-division-multiple-access-based cellular networks [18], the ICI was regarded as an additional source that deteriorates the performance, in addition to intracell interference among users, which is typically managed by spectrum spreading (i.e., interference averaging) and power control techniques [19]. In OFDM-based cellular networks, such as 3GPP LTE [20]; however, it has been observed that the ICI significantly degrades the system performance, and thus, many techniques are being proposed to mitigate the ICI for OFDM-based cellular networks [21]. Particularly in heterogeneous network environments, there may exist dominant interferers, which significantly affect adjacent cells [22]. Therefore, the ICI needs to be carefully managed in the OFDM-based multicell networks through efficient link adaptation and user scheduling algorithms.

Recently, there have been several studies on HARQ-based MU systems in the presence of interference. Narasimhan analyzed the throughput performance of the two-user interference channel with receiver cooperation [23]. Denic proposed a robust HARQ-incremental redundancy (IR) scheme in the presence of unknown interference such as jamming [24]. For multiple-input-multiple-output (MIMO)-based HARQ systems, several HARQ techniques were proposed by taking into account intercarrier interference and interantenna interference [25]–[27]. Rác *et al.* investigated an ICI coordination (ICIC) technique in the uplink 3GPP LTE system, considering HARQ techniques [28]. Makki *et al.* [29] proposed a coordinated HARQ scheme, which reallocates the spectrum of a successfully transmitted user to a user requiring subsequent retransmissions in cooperative multicell networks. Shirani-Mehr *et al.* proposed an optimal scheduling algorithm based on game theory in a MU-MIMO system with HARQ technique in the presence of ICI [30]. They investigated a joint optimization of user scheduling and transmit beamforming with HARQ in a distributed manner. To the best of our knowledge, however, there has been no such study that jointly investigates link adaptation and user scheduling with the HARQ technique in a multicell environment.

Manuscript received August 25, 2014; revised January 24, 2015; accepted March 13, 2015. Date of publication March 13, 2015; date of current version March 10, 2016. This work was supported by the Basic Science Research Program through the National Research Foundation of Korea (NRF) funded by the Ministry of Education under Grant 2013R1A1A2A10004905. The review of this paper was coordinated by Prof. C. Zhang. (Corresponding author: Bang Chul Jung.)

S. M. Kim was with the KTH Royal Institute of Technology, 114 28 Stockholm, Sweden, and also with Ericsson Research, 164 83 Stockholm, Sweden. He is now with the Department of Electronics Engineering, Korea Polytechnic University, Siheung 429-793, Korea (e-mail: suminkim@kpu.ac.kr).

B. C. Jung is with the Department of Electronics Engineering, Chungnam National University, Daejeon 305-764, Korea (e-mail: bangchuljung@gmail.com).

D. K. Sung is with the Department of Electrical Engineering, Korea Advanced Institute of Science and Technology, Daejeon 305-701, Korea (e-mail: dksung@ee.kaist.ac.kr).

Color versions of one or more of the figures in this paper are available online at <http://ieeexplore.ieee.org>.

Digital Object Identifier 10.1109/TVT.2015.2412693

In this paper, we investigate a joint link adaptation and user scheduling problem in a multicell downlink network, taking both HARQ and ICI into account. Main contributions of the paper are summarized as follows.

- A novel approximation model on the aggregated ICI at each user is proposed for enabling each base station (BS) to determine the optimal transmission rate, which assumes the dominant interfering terms at each user have identical path-loss statistics. Thus, we call this the identical path-loss approximation (IPLA) method. The effectiveness of IPLA is examined by comparing it with the conventional approximation method, i.e., Gaussian approximation (GA).
- An optimal rate selection (RS) algorithm with IPLA is proposed for maximizing the expected throughput of a single link in the multicell environment. Then, a simple but effective cross-layer framework is also proposed, which jointly combines link adaptation and user scheduling with the HARQ technique for the multicell environments.
- The performance of the proposed cross-layer framework is evaluated, in terms of cell throughput and user fairness, through extensive system-level simulations.

From the performance evaluation, it is shown that the well-known GA on ICI is not accurate in link adaptation and user scheduling with HARQ for multicell environments with some dominant interferers, while the proposed IPLA is highly accurate on the aggregated ICI, and thus, it provides an efficient joint link adaptation and user scheduling policy.

The rest of the paper is organized as follows: In Section II, the system model is introduced. In Section III, we propose an optimal link adaptation (transmission rate selection) algorithm for a single link by considering both the HARQ technique and the ICI. In Section IV, we propose a cross-layer framework jointly combining link adaptation and user scheduling and compares the proposed framework with the conventional strategies. In Section V, we show the performance of the proposed framework, in terms of cell throughput and fairness among users. Finally, we present concluding remarks in Section VI.

## II. SYSTEM MODEL

Fig. 1 illustrates the system model considered in this paper. We take into account a multicell downlink network, where there exist  $(K + 1)$  BSs with  $M$  transmit antennas and  $N$  users with a single receive antenna in each cell. Each BS is assumed to select a single user for data transmission in this paper for simplicity. In Fig. 1, the BS in the center, which is called the home cell, is denoted by superscript (0), and BSs in other cells are denoted by superscript  $(k)$ ,  $k \in \{1, \dots, K\}$ . Each BS selects a user within its coverage at each time slot (or scheduling interval) and transmits data with a *random beamforming* (RBF) technique, which is also called *opportunistic beamforming* (OBF) [31], [32]. As known in the literature, the RBF technique can achieve the system throughput with *true beamforming*, when a sufficiently large number of users exist in a cell, while it can significantly reduce the signaling overhead such as full CSI feedback for the true beamforming.

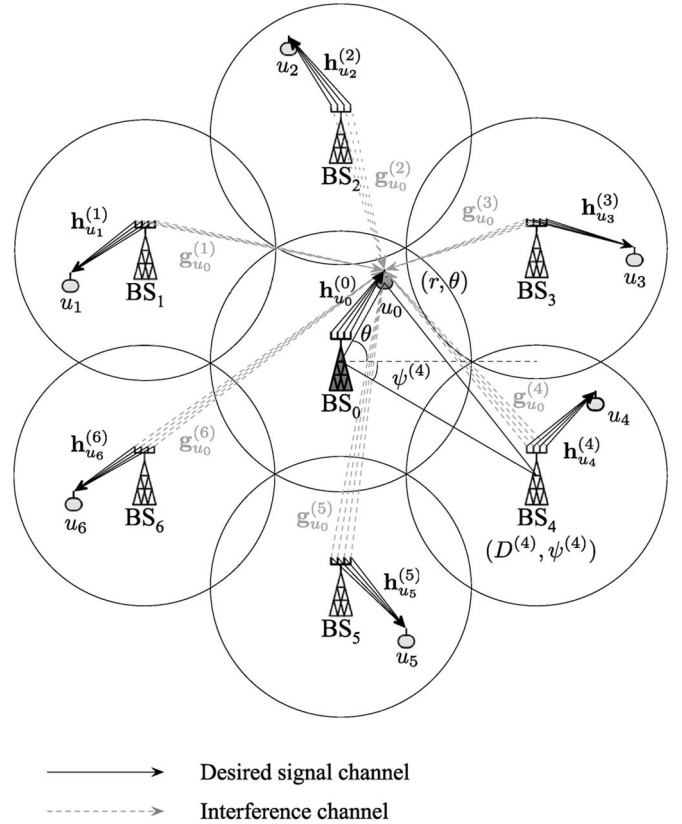


Fig. 1. System model.

The scheduled user in each cell receives a desired signal from its corresponding BS, and the ICI signals from  $K$  other-cell BSs. We focus on the user in the home cell, without loss of generality. The received signal of the scheduled user in the home cell (i.e.,  $k = 0$ ) is expressed as

$$y_{u_0}^{(0)} = \mathbf{h}_{u_0}^{(0)} \mathbf{v}_{u_0}^{(0)} x_{u_0}^{(0)} + \sum_{k=1}^K \mathbf{g}_{u_0}^{(k)} \mathbf{v}_{u_k}^{(k)} x_{u_k}^{(k)} + n_{u_0}^{(0)} \quad (1)$$

where  $u_k$  denotes the index of the selected user in the  $k$ th cell.  $\mathbf{h}_{u_0}^{(0)}$  and  $\mathbf{g}_{u_0}^{(k)}$  denote the channel vectors of the desired signal from the home cell (i.e.,  $k = 0$ ) and the interference signal from the  $k$ th cell, respectively.  $\mathbf{v}_{u_k}^{(k)}$  indicates the RBF vector for user  $u_k$  in the  $k$ th cell, and  $x_{u_k}^{(k)}$  represents the source data symbol of user  $u_k$  in the  $k$ th cell, and  $n_{u_0}^{(0)}$  denotes the additive white Gaussian noise, i.e.,  $n_{u_0}^{(0)} \sim \mathcal{CN}(0, N_0)$ , where  $N_0$  denotes the noise variance.

In (1),  $\mathbf{h}_{u_0}^{(0)}$  and  $\mathbf{g}_{u_0}^{(k)}$  denote the multiple-input–single-output channel vectors, including large-scale and small-scale fading components, i.e.,

$$\mathbf{h}_{u_0}^{(0)} \triangleq \left[ \sqrt{L_{u_0}^{(0)}} h_{u_0,1}^{(0)}, \sqrt{L_{u_0}^{(0)}} h_{u_0,2}^{(0)}, \dots, \sqrt{L_{u_0}^{(0)}} h_{u_0,M}^{(0)} \right] \quad (2)$$

$$\mathbf{g}_{u_0}^{(k)} \triangleq \left[ \sqrt{L_{u_0}^{(k)}} g_{u_0,1}^{(k)}, \sqrt{L_{u_0}^{(k)}} g_{u_0,2}^{(k)}, \dots, \sqrt{L_{u_0}^{(k)}} g_{u_0,M}^{(k)} \right] \quad (3)$$

where  $h_{u_0,m}^{(0)}$  and  $g_{u_0,m}^{(k)}$  denote the small-scale fading signal term of user  $u_0$  from the  $m$ th antenna of the home BS and the

$k$ th BS, respectively, and they are assumed to follow a circular symmetric complex Gaussian distribution with zero mean and unit variance, i.e.,  $h_{u_0,m}^{(0)} \sim \mathcal{CN}(0, 1)$  and  $g_{u_0,m}^{(k)} \sim \mathcal{CN}(0, 1)$  for  $m = \{1, \dots, M\}$ . We assume a slowly varying channel condition, and thus,  $h_{u_0,m}^{(0)}$  and  $g_{u_0,m}^{(k)}$  are quasi-static during a single HARQ retransmission process.  $L_{u_0}^{(0)}$  and  $L_{u_0}^{(k)}$  denote the large-scale fading power terms regarded as path loss of user  $u_0$  from the home BS and the  $k$ th BS, respectively.  $L_{u_0}^{(k)}$  is given by  $10^{-(\text{PL}_0/10)} \cdot (d_0/d_{u_0}^{(k)})^\alpha$ , ( $k = 0, \dots, K$ ), where  $\text{PL}_0$  denotes the path loss (in decibels) at reference distance  $d_0$ ,  $\alpha$  denotes the path-loss exponent, and  $d_{u_0}^{(k)}$  represents the distance between user  $u_0$  and the  $k$ th BS. When user and BS locations in the home cell are given by  $(r, \theta)$  and  $(D^{(k)}, \psi^{(k)})$ ,  $d_{u_0}^{(k)}$  can be calculated by  $\sqrt{r^2 + (D^{(k)})^2 - 2rD^{(k)} \cos(\theta - \psi^{(k)})}$ , ( $k = 0, \dots, K$ ), where  $D^{(0)} = 0$  (i.e.,  $d_{u_0}^{(0)} = r$ ). In general, since BSs are deployed at fixed locations in advance, the home BS can easily know the location information of neighboring BSs. Additionally, we assume that the home BS also knows the user location information through periodic measurement or feedback from the user. The 3GPP LTE system has already been supporting several user positioning methods, even if GPS signal is unavailable [33]. Since we assume the perfect positioning in this paper, the performance can be degraded when the estimated user location is imperfect. The effect of position estimation error is beyond the scope of this paper.

Since the RBF scheme is considered as in [31], the beamforming vectors in (1) are obtained by  $\mathbf{v}_{u_k}^{(k)} = [v_{u_k,1}^{(k)}, v_{u_k,2}^{(k)}, \dots, v_{u_k,M}^{(k)}]^T$ , ( $k = 0, \dots, K$ ), where  $[\cdot]^T$  denotes the transpose of a vector;  $v_{u_k,m}^{(k)} = \sqrt{a_m} e^{j\theta_m}$ , where  $a_m \in [0, 1]$ ,  $\theta_m \sim \text{Uniform}[-\pi, \pi]$ ; and  $\|\mathbf{v}_{u_k}^{(k)}\|^2 = \sum_{m=1}^M a_m = 1$ . Through a property of the RBF scheme, the second term in (1), i.e., the sum of ICI terms, is derived by

$$\begin{aligned} \mathcal{I} &= \sum_{k=1}^K \mathbf{g}_{u_0}^{(k)} \mathbf{v}_{u_k}^{(k)} x_{u_k}^{(k)} \\ &= \sum_{k=1}^K \sqrt{L_{u_0}^{(k)}} \left( g_{u_0,1}^{(k)} v_{u_k,1}^{(k)} + \dots + g_{u_0,M}^{(k)} v_{u_k,M}^{(k)} \right) x_{u_k}^{(k)} \\ &= \sum_{k=1}^K \sqrt{L_{u_0}^{(k)}} \left( \underbrace{\sqrt{\alpha_1} e^{j\theta_1} g_{u_0,1}^{(k)} + \dots + \sqrt{\alpha_M} e^{j\theta_M} g_{u_0,M}^{(k)}}_{\sim \mathcal{CN}(0,1)} \right) x_{u_k}^{(k)} \\ &= \sum_{k=1}^K \sqrt{L_{u_0}^{(k)}} w_{u_0}^{(k)} x_{u_k}^{(k)} \end{aligned} \quad (4)$$

where  $w_{u_0}^{(k)} \sim \mathcal{CN}(0, 1)$ , and the last equality is derived from an isotropic property of a complex Gaussian random variable [7].

Consequently, the received SINR of the scheduled user in the home cell is

$$\gamma = \frac{s}{\mathcal{X} + 1/\rho} \quad (5)$$

where  $s = \|\mathbf{h}_{u_0}^{(0)} \mathbf{v}_{u_0}^{(0)}\|^2 = L_{u_0}^{(0)} |w_{u_0}^{(0)}|^2$ ,  $\mathcal{X} = \sum_{k=1}^K L_{u_0}^{(k)} |w_{u_0}^{(k)}|^2$ , and  $\rho = P_x/N_0$ , where  $\mathbb{E}[|x_{u_k}^{(k)}|^2] = P_x$  for  $k = \{0, \dots, K\}$ . Here,  $L_{u_0}^{(0)}$  is a known constant based on user location information at the home BS, and we assume that the effective channel power gain of  $u_0$ , i.e.,  $|w_{u_0}^{(0)}|^2$ , is perfectly known at the transmitter (i.e., home BS). It is reasonable because the home BS knows the RBF vector (i.e.,  $\mathbf{v}_{u_0}^{(k)}$ ) for user  $u_0$  in advance, and we consider a quasi-static channel condition where it is possible to estimate the effective channel power gain perfectly for the desired signal channel (i.e.,  $\mathbf{h}_{u_0}^{(0)}$ ). Hence, the desired signal power term  $s$  is a known constant at the transmitter. Furthermore, the inverse of the transmit SNR term is negligible in an interference-limited regime (i.e., the high-SNR regime).

Throughout this paper, we consider the chase-combining-based HARQ (HARQ-CC) protocol, in which every retransmitted information is same as the one at the initial transmission. The HARQ-CC protocol is simple but obtains a sufficient benefit of HARQ from the combined power gain. Thus, it is widely used in practical wireless communication systems.

### III. OPTIMAL RATE SELECTION FOR A SINGLE LINK

Here, we first mathematically formulate the effective SINR and the delay-limited throughput (DLT), which represents an expected throughput, under a given maximum allowable number of transmissions in HARQ-based systems [8], [9], [11] and [34]. Then, we consider a well-known GA on the ICI with noise at users. Finally, we propose an IPLA on the aggregated ICI term at users. We also obtain the optimal transmission rate maximizing the DLT for both approximation methods.

#### A. Effective SINR and DLT

First, the effective SINR after the  $n$ th transmission attempt after HARQ-CC<sup>1</sup> combining becomes

$$\gamma(n) = \sum_{i=1}^n \gamma_i = \sum_{i=1}^n \frac{s}{\mathcal{X}_i + 1/\rho} \quad (6)$$

where  $\gamma_i$  represents the received SINR at the  $i$ th transmission;  $\mathcal{X}_i$  denotes the ICI power at the  $i$ th transmission, which is expressed as  $\mathcal{X}_i = \sum_{k=1}^K L_{u_0}^{(k)} |w_{u_0}^{(k)}(t_i)|^2$ , where  $t_i$  indicates the time slot index of the  $i$ th transmission; and  $s = L_{u_0}^{(0)} |w_{u_0}^{(0)}(t_i)|^2 = L_{u_0}^{(0)} |w_{u_0}^{(0)}(t_1)|^2$  denotes the desired signal power. Since the RBF vector is kept during retransmissions and the desired signal channel is quasi-static during retransmissions,  $s$  is a known constant for every (re)transmission of a single packet. In contrast, beamforming vectors (i.e.,  $\mathbf{v}_{u_k}^{(k)}$ ) in other cells are independently varying according to scheduling decisions by other-cell BSs, although interference channel vectors  $\mathbf{g}_{u_0}^{(k)}$  are quasi-static during their own retransmission processes. More specifically, new users can be scheduled after their own transmission successes in other cells during retransmissions in the home cell. This causes asynchronous scheduling among different cells, which implies that different cells suffer

<sup>1</sup>The HARQ-CC has been widely adopted in 3GPP HSPA [35], WiMAX [36], 3GPP LTE [20], and their evolutions.

from different user scheduling instances. Accordingly, the aggregated ICI term is independently varying for every (re)transmission, due to the independently varying other-cell beamforming vectors.

Next, the distribution of the effective SINR needs to be analyzed for transmission rate selection. We start to derive the distribution of the effective SINR based on numerical inversion of characteristic function (CF) from the following lemma.

**Lemma 1 (Inversion Formula of Gil-Pelaez [37]):** Let  $\phi(t) = \int_{-\infty}^{\infty} e^{jtx} dF(x)$  be a CF of the 1-D distribution function  $F(x)$ . For  $x$  being the continuity point of the distribution, the following inversion formula holds true:

$$\begin{aligned} F(x) &= \frac{1}{2} - \frac{1}{\pi} \int_0^{\infty} \left( \frac{e^{-jtx}\phi(t) - e^{jtx}\phi(-t)}{2jt} \right) dt \\ &= \frac{1}{2} - \frac{1}{\pi} \int_0^{\infty} \mathcal{Im} \left( \frac{e^{-jtx}\phi(t)}{t} \right) dt \end{aligned} \quad (7)$$

where  $\mathcal{Im}\{\cdot\}$  denotes the imaginary part of a complex number.

*Proof:* See [37]. ■

By using Lemma 1, if we know the CF of the effective SINR after the  $n$ th (re)transmission, which is denoted by  $\phi_{\gamma(n)}(t)$ , we can obtain the cumulative distribution function (CDF)  $F_{\gamma(n)}(x)$ . Assuming the information-theoretic capacity-achieving channel coding scheme, the outage probability after the  $n$ th (re)transmission is defined by

$$P_{\text{out}}(n, R) \triangleq \Pr \{ \log_2(1 + \gamma(n)) < R \} = F_{\gamma(n)}(2^R - 1) \quad (8)$$

where  $R$  denotes the required transmission source rate. Then, the DLT is obtained by [11]

$$S(R) \triangleq \sum_{i=1}^{N_{\max}} \frac{R}{i} [P_{\text{out}}(i-1, R) - P_{\text{out}}(i, R)] \quad (9)$$

where  $N_{\max}$  denotes the maximum allowable number of transmissions in an HARQ retransmission process. Substituting (7) and (8) for (9), the DLT is finally rewritten as

$$\begin{aligned} S(R) &= \sum_{i=1}^{N_{\max}} \frac{R}{i \cdot \pi} \\ &\cdot \int_0^{\infty} \left[ \mathcal{Im} \left\{ \frac{e^{-jt(2^R-1)}}{t} \cdot (\phi_{\gamma(i)}(t) - \phi_{\gamma(i-1)}(t)) \right\} \right] dt. \end{aligned} \quad (10)$$

### B. Link Adaptation With GA

Traditionally, the sum of ICI terms is widely approximated as a Gaussian distribution by the well-known central limit theorem (CLT) for even six interference components considering seven-cell-structured cellular networks [38], [39]. Therefore, we investigate a RS scheme, assuming that the ICI plus noise term follows a Gaussian distribution as a conventional link adaptation scheme. Through the GA, the effective SINR after HARQ-CC combining can be approximated by

$$\gamma(n) = \sum_{i=1}^n \frac{s}{\mathcal{X}_i + 1/\rho} \approx \sum_{i=1}^n \tilde{\gamma}_i = \sum_{i=1}^n \frac{s}{|Z_i|^2} \quad (11)$$

where  $Z_i$  denotes a complex Gaussian random variable with zero mean and variance of the sum of ICI and noise powers, i.e.,  $Z_i \sim \mathcal{CN}(0, \sigma_Z^2)$ , where  $\sigma_Z^2 = \sum_{k=1}^K L_{u_0}^{(k)} + 1/\rho$ , and  $s = L_{u_0}^{(0)} |w_{u_0}^{(0)}(t_1)|^2$ . Here,  $\tilde{\gamma}_i$  is an inverted Gamma random variable with shape parameter 1 and scale parameter  $s/\sigma_Z^2$ , i.e.,  $\tilde{\gamma}_i \sim \text{Inv-Gamma}(1, s/\sigma_Z^2)$ .

First, the PDF of  $\tilde{\gamma}_i$  by the GA is

$$f_{\tilde{\gamma}_i}(x) = \left( \frac{s}{\sigma_Z^2} \right) x^{-2} e^{-s/(\sigma_Z^2 x)}. \quad (12)$$

To derive the distribution of sum of  $\tilde{\gamma}_i$  (i.e.,  $\gamma(n)$ ), the CF of  $\tilde{\gamma}_i$  is derived first as follows [40]:

$$\phi_{\tilde{\gamma}_i}(t) = \sqrt{-\frac{4jst}{\sigma_Z^2}} K_1 \left( \sqrt{-\frac{4jst}{\sigma_Z^2}} \right) \quad (13)$$

where  $K_\nu(\cdot)$  denotes the modified Bessel function of the second kind. Since  $\tilde{\gamma}_i$  are identically and independently distributed (i.i.d.) random variables due to independently varying  $\mathcal{X}_i$ , the CF of  $\gamma(n)$  is obtained by

$$\phi_{\gamma(n)}(t) = \prod_{i=1}^n \phi_{\tilde{\gamma}_i}(t) = \left[ \sqrt{-\frac{4jst}{\sigma_Z^2}} K_1 \left( \sqrt{-\frac{4jst}{\sigma_Z^2}} \right) \right]^n. \quad (14)$$

By substituting (14) for (10), the DLT of the conventional GA is obtained by

$$\begin{aligned} S_{\text{GA}}(R) &= \sum_{i=1}^{N_{\max}} \frac{R}{i \cdot \pi} \\ &\cdot \int_0^{\infty} [\mathcal{Im} \{ \Psi_{\text{GA}}(t; i, R) - \Psi_{\text{GA}}(t; i-1, R) \}] dt \end{aligned} \quad (15)$$

where

$$\Psi_{\text{GA}}(t; i, R) = \frac{e^{-jt(2^R-1)}}{t} \left[ \sqrt{-\frac{4jst}{\sigma_Z^2}} K_1 \left( \sqrt{-\frac{4jst}{\sigma_Z^2}} \right) \right]^i.$$

Finally, the optimal source rate for maximizing the DLT through the conventional GA is determined by

$$\begin{aligned} R_{\text{GA}}^* &= \arg \max_{R \geq 0} \sum_{i=1}^{N_{\max}} \frac{R}{i \cdot \pi} \\ &\cdot \int_0^{\infty} [\mathcal{Im} \{ \Psi_{\text{GA}}(t; i, R) - \Psi_{\text{GA}}(t; i-1, R) \}] dt. \end{aligned} \quad (16)$$

### C. Link Adaptation With IPLA

Assuming the interference-limited regime (i.e.,  $\rho \gg 1$ ), the effective SINR after HARQ-CC combining can be approximated by

$$\gamma(n) \approx \sum_{i=1}^n \frac{s}{\mathcal{X}_i} = \sum_{i=1}^n \frac{s}{\sum_{k=1}^K L_{u_0}^{(k)} |w_{u_0}^{(k)}(t_i)|^2} \quad (17)$$

where  $t_i$  denotes the time slot index of the  $i$ th transmission, and  $s = L_{u_0}^{(0)} |w_{u_0}^{(0)}(t_1)|^2$ . The sum of ICI terms in the denominator of (17) is a weighted sum of Gamma random variables since  $w_{u_0}^{(k)}(t_i) \sim \mathcal{CN}(0, 1)$  and  $L_{u_0}^{(k)} \neq L_{u_0}^{(l)}$  for  $k \neq l \in \{1, \dots, K\}$ . Note that there exists no closed-form expression for such distribution, although there have been some efforts to develop computational methods [41], [42]. Furthermore, the distribution of the effective SINR after the  $n$ th transmission attempt, i.e.,  $\gamma(n)$ , which is the sum of the inverse of the weighted sum of Gamma random variables, has a much more complicated form, and therefore, it is intractable to derive its CF mathematically. Since only the contribution of the aggregated ICI, rather than individual ICIs, is interested in the effective SINR and even nondominant interferers cannot be simply negligible,<sup>2</sup> we propose to approximate all path-loss terms from other-cell BSs to be identical as their average value. Then, the effective SINR can be approximated by

$$\gamma(n) \approx \sum_{i=1}^n \tilde{\gamma}_i = \sum_{i=1}^n \frac{s}{\sum_{k=1}^K \bar{L} |w_{u_0}^{(k)}(t_i)|^2} \quad (18)$$

where  $\bar{L} = (1/K) \sum_{k=1}^K L_{u_0}^{(k)}$  denotes the average value of all path-loss terms from other cells. It is worth noting that the proposed IPLA preserves the average statistics of the aggregated ICI since for a given user,  $\mathbb{E}[\sum_{k=1}^K \bar{L} |w_{u_0}^{(k)}(t_i)|^2] = \bar{L} \mathbb{E}[\sum_{k=1}^K |w_{u_0}^{(k)}(t_i)|^2] = \bar{L} \sum_{k=1}^K \mathbb{E}[|w_{u_0}^{(k)}(t_i)|^2] = \bar{L} K = \sum_{k=1}^K L_{u_0}^{(k)}$ , while  $\mathbb{E}[\sum_{k=1}^K L_{u_0}^{(k)} |w_{u_0}^{(k)}(t_i)|^2] = \sum_{k=1}^K L_{u_0}^{(k)} \mathbb{E}[|w_{u_0}^{(k)}(t_i)|^2] = \sum_{k=1}^K L_{u_0}^{(k)}$  because  $L_{u_0}^{(k)}$  are deterministic for the given user.

Now, the sum of ICI terms becomes the sum of i.i.d. Gamma random variables, and it also follows a Gamma distribution. After all, the approximated SINR at the  $i$ th transmission, i.e.,  $\tilde{\gamma}_i$ , follows an inverted Gamma distribution, i.e.,  $\tilde{\gamma}_i \sim \text{Inv-Gamma}(K, s/\bar{L})$ . Hence, the probability density function of  $\tilde{\gamma}_i$  is

$$f_{\tilde{\gamma}_i}(x) = \frac{\left(\frac{s}{\bar{L}}\right)^K}{(K-1)!} x^{-K-1} e^{-s/(\bar{L}x)}. \quad (19)$$

Then, the CF of  $\tilde{\gamma}_i$  and  $\gamma(n)$  are derived, respectively, as follows [40]:

$$\begin{aligned} \phi_{\tilde{\gamma}_i}(t) &= \frac{2 \left(-\frac{jst}{\bar{L}}\right)^{\frac{K}{2}}}{(K-1)!} K_K \left( \sqrt{-\frac{4jst}{\bar{L}}} \right) \\ \phi_{\gamma(n)}(t) &= \prod_{i=1}^n \phi_{\tilde{\gamma}_i}(t) = \left[ \frac{2 \left(-\frac{jst}{\bar{L}}\right)^{\frac{K}{2}}}{(K-1)!} K_K \left( \sqrt{-\frac{4jst}{\bar{L}}} \right) \right]^n \end{aligned} \quad (20)$$

where  $K_\nu(\cdot)$  denotes the modified Bessel function of the second kind. By substituting (21) for (10), the DLT by the proposed

IPLA is

$$S_{\text{IPLA}}(R) = \sum_{i=1}^{N_{\max}} \frac{R}{i \cdot \pi} \cdot \int_0^\infty [\text{Im}\{\Psi_{\text{IPLA}}(t; i, R) - \Psi_{\text{IPLA}}(t; i-1, R)\}] dt \quad (22)$$

where

$$\Psi_{\text{IPLA}}(t; i, R) = \frac{e^{-jt(2^R-1)}}{t} \left[ \frac{2 \left(-\frac{jst}{\bar{L}}\right)^{\frac{K}{2}}}{(K-1)!} K_K \left( \sqrt{-\frac{4jst}{\bar{L}}} \right) \right]^i.$$

Eventually, the optimal source rate based on the proposed IPLA for maximizing the DLT is determined by

$$R_{\text{IPLA}}^* = \underset{R \geq 0}{\text{argmax}} \sum_{i=1}^{N_{\max}} \frac{R}{i \cdot \pi} \cdot \int_0^\infty [\text{Im}\{\Psi_{\text{IPLA}}(t; i, R) - \Psi_{\text{IPLA}}(t; i-1, R)\}] dt. \quad (23)$$

The aforementioned optimal source rate can be easily found by a grid search or a Golden section search, with range between zero and a proper upper limit, since the DLT has a shape of quasi-concave function with respect to the source rate, as shown numerically in Section V-B, although it cannot be analytically proved due to a sophisticated form of the DLT formula.

#### IV. JOINT LINK ADAPTATION AND USER SCHEDULING: CROSS-LAYER FRAMEWORK

##### A. Overall Procedure

We first propose a simple cross-layer framework to perform both link adaptation and user scheduling, considering HARQ and ICI. The cross-layer framework consists of three main components: RS, *effective rate mapping* (ERM), and *scheduler*. The roles of components are described as in the following.

1) *RS*: The RS plays a role to determine an optimal transmission source rate  $R_u^*(t)$  for the  $u$ th user at the initial transmission instance of the HARQ-based system. In this paper, we consider RS schemes to maximize the DLT of each user considering HARQ retransmission and ICI statistics, as presented in the previous section.

2) *ERM*: The transmission source rate is different from the achievable rate in HARQ-based systems due to uncertain retransmissions. Therefore, an effective rate, which is close to the achievable rate, needs to be taken into account for user scheduling, if it is available. The ERM determines an effective rate  $R_{\text{eff},u}(t)$  for the  $u$ th user as a function of the optimal source rate  $R_u^*(t)$ , i.e.,  $R_{\text{eff},u}(t) = f(R_u^*(t))$ , to adjust the scheduling priority of each user. Through such ERM, the instantaneous rate  $R_u(t)$  in the scheduler is replaced by the effective rate  $R_{\text{eff},u}(t)$ . After all, the scheduler selects a user with the highest utility value substituted into the effective rate.

3) *Scheduler*: The scheduler determines which user is the best at every scheduling instance. There are three representative

<sup>2</sup>To validate this statement, we examine the expected throughput of taking three dominant interferers among whole interferers, as compared with the exact one in Section V-B.

scheduling algorithms: *Round Robin*, *Max C/I*, and *Proportional Fair* (PF). In this paper, we take into account the PF scheduler for an asymmetric user distribution scenario, where users have different distances from the BS, to consider user fairness. The PF scheduler is simply expressed as

$$u^* = \arg \max_{u \in \Pi} \frac{R_u(t)}{T_u(t)} \quad (24)$$

where  $\Pi$  denotes the set of users in a cell;  $R_u(t)$  denotes the achievable rate of the  $u$ th user at time slot  $t$ ; and  $T_u(t)$  denotes the average throughput of the  $u$ th user at time slot  $t$ , which is updated as  $T_u(t+1) = (1 - (1/t_c)) \cdot T_u(t) + (1/t_c) \cdot R_u(t) \cdot \mathbb{I}\{u = u^*\}$ , where  $t_c$  denotes the predetermined windowing interval for moving averaging, and  $\mathbb{I}\{x\}$  denotes the indication function, which is one if  $x$  is true and zero otherwise. In the HARQ-based systems,  $R_u(t)$  should be modified, considering the HARQ retransmission process, and it can be done by the ERM in this cross-layer framework.

The operating procedure according to the proposed cross-layer framework is illustrated as follows.

(Step 1) **[Rate Selection]**: Determine  $R_u^*(t)$   
 (Step 2) **[Effective Rate Mapping]**:  
     Determine  $R_{\text{eff},u}(t) = f(R_u^*(t))$   
 (Step 3) **[Scheduler]**: Determine  $u^* = \arg \max_{u \in \Pi} R_{\text{eff},u}(t)/T_u(t)$   
 (Step 4) **[HARQ Transmission]**  
     –  $u^*$  transmits with  $R_u^*(t)$  until successful transmission or maximum transmission limit.  
     – Go to (Step 1) for all users after the end of the (re)transmissions of the scheduled user  $u^*$ .

### B. Proposed Cross-Layer Policy and Other Candidates

Here, we propose an IPLA-based cross-layer policy. We also introduce two reference and two conventional policies for the performance comparison in the next section. Hereafter, each cross-layer policy is denoted by the RS and ERM, i.e.,  $\mathcal{P}\{\text{RS}, \text{ERM}\}$ , since all policies employ the same PF scheduler.

1) *Proposed IPLA-Based Policy*  $\mathcal{P}\{\text{RS-IPLA}, S_{\text{IPLA}}(R_{\text{IPLA}}^*)\}$ : The proposed IPLA-based policy is based on RS through the IPLA on the aggregated ICI term (so-called RS-IPLA). According to the RS-IPLA proposed in the previous section, the transmission source rate of the  $u$ th user is determined by (23). Since it takes into account an HARQ retransmission process using statistics of the aggregated ICI term, which is assumed by a Gamma distribution through the IPLA, the achievable rate is different from the transmission source rate. Thus, the *expected throughput*-based ERM is considered for user scheduling as

$$R_{\text{eff},u} = S_{\text{IPLA}}(R_{\text{IPLA},u}^*) = \sum_{i=1}^{N_{\max}} \frac{R_{\text{IPLA},u}^*}{i \cdot \pi} \int_0^{\infty} [\mathcal{I}m\{\Phi_{\text{IPLA}}(t; i, R_{\text{IPLA},u}^*) - \Phi_{\text{IPLA}}(t; i-1, R_{\text{IPLA},u}^*)\}] dt \quad (25)$$

where

$$\Phi_{\text{IPLA}}(t; i, R_{\text{IPLA},u}^*) = \frac{e^{-jt(2^{R_{\text{IPLA},u}^*} - 1)}}{t} \cdot \left[ \frac{2 \left(-\frac{jst}{L}\right)^{\frac{K}{2}}}{(K-1)!} \cdot K_K \left( \sqrt{-\frac{4jst}{L}} \right) \right]^i.$$

Based on the selected transmission source rate and effective rate, the user scheduling is performed with the PF criterion, and then, the HARQ transmission is performed for the scheduled user, according to (Step 4) in the operating procedure of the cross-layer framework.

#### 2) Reference Policies:

##### • *Genie-Aided Policy* $\mathcal{P}\{\text{RS-Opt}, R_{\text{Opt}}^*\}$

The genie-aided policy has perfect knowledge on instantaneous ICI terms. In this case, the transmitter can accurately adapt to instantaneous interference channel, and the channel capacity depending on the instantaneous interference channel conditions is achieved with no retransmission and outage. Although this policy is rather unrealistic, it offers an upper bound of the system performance. According to the RS-Opt scheme with the perfect knowledge for interference channels, the transmission source rate of the  $u$ th user is determined by

$$R_{\text{Opt},u}^* = \log_2 \left( 1 + \frac{s}{\sum_{k=1}^K L_u^{(k)} |w_u^{(k)}(t_1)|^2 + 1/\rho} \right) \quad (26)$$

where  $t_1$  denotes the time index at initial transmission,  $|w_u^{(k)}(t_1)|^2$  represents the exact effective interference channel power gain from the  $k$ th BS to the  $u$ th user in the home cell,  $s = L_u^{(0)} |w_u^{(0)}(t_1)|^2$ , and  $\rho = P_x/N_0$ . Next, since the genie-aided policy does not cause outage and retransmission, the *instantaneous rate*-based ERM is considered as

$$R_{\text{eff},u} = R_{\text{Opt},u}^* \quad (27)$$

##### • *Instantaneous SINR Policy* $\mathcal{P}\{\text{RS-}i\text{-SINR}, R_{i\text{-SINR}}^*\}$

The instantaneous SINR policy is the simplest one based on the SINR value fed back from the receiver. This policy has inaccurate RS, due to independently varying interference channels for every (re)transmission and a feedback delay. According to the RS- $i$ -SINR scheme using the outdated feedback channel information, the transmission source rate of the  $u$ th user is determined by

$$R_{i\text{-SINR},u}^* = \log_2 \left( 1 + \frac{s}{\sum_{k=1}^K L_u^{(k)} |w_u^{(k)}(t_1 - \delta)|^2 + 1/\rho} \right) \quad (28)$$

where  $|w_u^{(k)}(t_1 - \delta)|^2$  represents the interference power gain from the  $k$ th BS to user  $u$  with the feedback delay  $\delta$ ,  $s = L_u^{(0)} |w_u^{(0)}(t_1)|^2$ , and  $\rho = P_x/N_0$ . Since the

instantaneous SINR policy takes advantage of only instantaneous information without consideration of HARQ retransmission, the *instantaneous rate*-based ERM is also considered as

$$R_{\text{eff},u} = R_{i\text{-SINR},u}^* \quad (29)$$

### 3) Conventional Policies:

- *Average Interference Policy*  $\mathcal{P}\{\text{RS-Avg-}\mathcal{X}, R_{\text{Avg-}\mathcal{X}}^*\}$   
The average interference policy exploits an average value for the aggregated ICI term [26], since each ICI term is an uncertain and independently varying factor. According to the RS-Avg- $\mathcal{X}$  scheme replacing the aggregated ICI term by the average value, the transmission source rate of the  $u$ th user is determined by

$$R_{\text{Avg-}\mathcal{X},u}^* = \log_2 \left( 1 + \frac{s}{\bar{\mathcal{X}} + 1/\rho} \right) \quad (30)$$

where  $\bar{\mathcal{X}} = \mathbb{E} \left[ \sum_{k=1}^K L_u^{(k)} |w_u^{(k)}|^2 \right] = \sum_{k=1}^K L_u^{(k)}$ ,  $s = L_u^{(0)} |w_u^{(0)}(t_1)|^2$ , and  $\rho = P_x/N_0$ . The average interference policy has an identical source rate during retransmissions because of applying the average value for the sum of ICI terms. Thus, similar to (27) and (29), the *instantaneous rate*-based ERM is considered as

$$R_{\text{eff},u} = R_{\text{Avg-}\mathcal{X},u}^* \quad (31)$$

- *GA-based Policy*  $\mathcal{P}\{\text{RS-GA}, S_{\text{GA}}(R_{\text{GA}}^*)\}$   
The GA-based policy is based on RS through GA for the sum of ICI and noise terms. According to the RS-GA scheme investigated in the previous section, the transmission source rate of the  $u$ th user is determined by (16). Since the GA-based policy considers an HARQ retransmission process using statistics of the aggregated ICI term, the *expected throughput*-based ERM is considered as

$$R_{\text{eff},u} = S_{\text{GA}}(R_{\text{GA},u}^*) = \sum_{i=1}^{N_{\text{max}}} \frac{R_{\text{GA},u}^*}{i \cdot \pi} \cdot \int_0^\infty [\text{Im} \{ \Phi_{\text{GA}}(t; i, R_{\text{GA},u}^*) - \Phi_{\text{GA}}(t; i-1, R_{\text{GA},u}^*) \}] dt \quad (32)$$

where

$$\Phi_{\text{GA}}(t; i, R_{\text{GA},u}^*) = \frac{e^{-jt(2^{R_{\text{GA},u}^*} - 1)}}{t} \cdot \left[ \sqrt{-\frac{4jst}{\sigma_Z^2}} \cdot K_1 \left( \sqrt{-\frac{4jst}{\sigma_Z^2}} \right) \right]^i.$$

## V. NUMERICAL RESULTS

Here, we first examine the effectiveness of the proposed IPLA through a quantile-versus-quantile (Q-Q) plot on the effective SINR distribution  $F_{\gamma(n)}(x)$ . After this, we discuss the

effects of user distance and path-loss exponent on the RS in a single link. Finally, we evaluate the performance of the proposed, conventional, and reference cross-layer policies, in terms of system throughput and fairness metric, through system-level simulations. As basic simulation setups, we consider a one-tier cellular network with six other cells (i.e.,  $K = 6$ ), where users are asymmetrically distributed in the home cell. The BS-to-BS distance is set to 1000 m (i.e.,  $D^{(k)} = 1000 \forall k$ ), and angles between BS in the home cell and BSs in the other cells are set to  $\psi^{(k)} = (5\pi/6) - (k\pi/3)$ , i.e.,  $\vec{\psi} = [5\pi/6, \pi/2, \pi/6, -\pi/6, -\pi/2, -5\pi/6]$ . We set the distances between users and the home BS to  $r \in [150, 200, 250, 300, 400]$  m, and each element in the vector is equally set according to the number of users. Therefore, we just consider the number of users as multiple of five, and this is 250 m for a single-user case. Additionally, the angles between users and the home BS are uniformly determined as  $\theta = \text{Uniform}[-\pi, \pi]$ . For path loss, we set  $\text{PL}_0$  to 37 dB, at reference distance  $d_0 = 1000$  m, and path-loss exponent  $\alpha$  to 3. The maximum allowable number of transmissions  $N_{\text{max}}$  is set to 4, which is a typical value in LTE and WiMAX systems. To take into account an interference-limited situation, we set transmit SNR  $\rho$  to 43 dB.<sup>3</sup>

### A. Statistical Distribution of Effective SINR Based on IPLA

To examine the effectiveness of the proposed IPLA, we introduce a Q-Q plot, which is widely used for quantitative comparison between two distributions. It can provide an intuitive comparison between two statistical data sets, as well as two theoretical distributions, and more information on the local agreement between two distributions than other fitting tests, such as chi-square and Kolmogorov-Smirnov tests [43]. In this paper, we compare two theoretically approximated distributions with the real empirical distribution. In the Q-Q plot, the  $x$ -axis is based on the theoretical distribution with the approximated CDF, which is obtained by inverting the CDF, i.e.,  $F_{\gamma(n)}^{-1}(x)$ , and the  $y$ -axis is based on the empirical quantile from a sample data set on the effective SINR obtained by statistical realizations.

Fig. 2 shows the Q-Q plots of the proposed IPLA and the conventional GA compared with the real empirical distribution, according to the number of transmission attempts of a single packet, i.e.,  $n$ . Since the line  $y = x$  represents the identity of two compared distributions in the Q-Q plot, the proposed IPLA almost following the  $y = x$  line agrees well with the real empirical distribution, regardless of  $n$  values. As a general trend, with increasing the number of transmission attempts  $n$ , the Q-Q plots of both approximated distributions move to the upper right side, which implies a larger effective SINR value due to an HARQ-CC combining gain. While the Q-Q plot of the proposed IPLA agrees well, that of the conventional GA is flatter than the line  $y = x$ . This implies that the approximated distribution by the GA is more dispersed than the real empirical distribution. Additionally, the difference between the approximated distribution by the GA and the empirical distribution increases as the value of effective SINR increases. Through the

<sup>3</sup>In this setting, the average received SNR without interference becomes 6 dB when the distance is 1000 m.

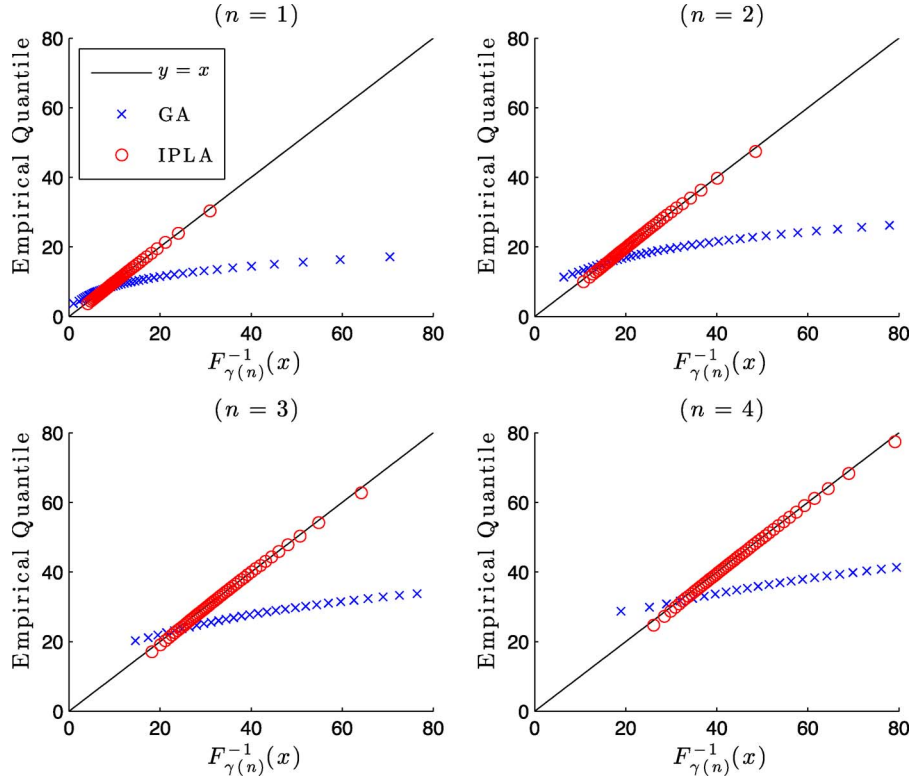


Fig. 2. Q-Q plots of the proposed IPLA and the conventional GA ( $K = 6$ ,  $r = 250$  m,  $\theta = \pi/2$ ,  $\alpha = 3$ ,  $|w_{u_0}^{(0)}|^2 = 1$ , and  $N_{\max} = 4$ ).

comparison of the approximated distributions with the real empirical distribution, it is shown that the proposed IPLA offers a good approximation on the effective SINR, while the conventional GA gives significant differences in the approximation.

#### B. Link Adaptation for a Single Link: Effects of User Distance and Path-Loss Exponent

Here, we investigate the effects of user distance and path-loss exponent on the RS, according to the proposed and conventional link adaptation schemes. Fig. 3 shows the DLT for varying source rate  $R$  in three different user-distance values. Basically, the DLT has a shape of quasi-concave function and a single optimal point, with respect to the source rate. As the distance decreases, a higher DLT is achieved since the desired signal power increases, while a closer distance to the BS fundamentally yields smaller interference from other-cell BSs. In the figure, the solid lines denote the exact simulation results with perfectly known individual ICIs. Additionally, the dotted lines denote the simulation results with three perfectly known dominant ICIs, which neglect the other three ICIs. Compared to both simulation results, neglecting nondominant ICIs yields overestimated DLTs, due to the reduced interference, even if it shows similar shapes of curves. On the contrary, the DLT analytically derived by the proposed IPLA has a high similarity with the one by the exact simulation for all distance values. After all, the optimal source rate determined by the proposed IPLA is approximately identical to the actual optimal source rate on the exact simulation curves, regardless of the user distances. However, optimal source rates based on the two

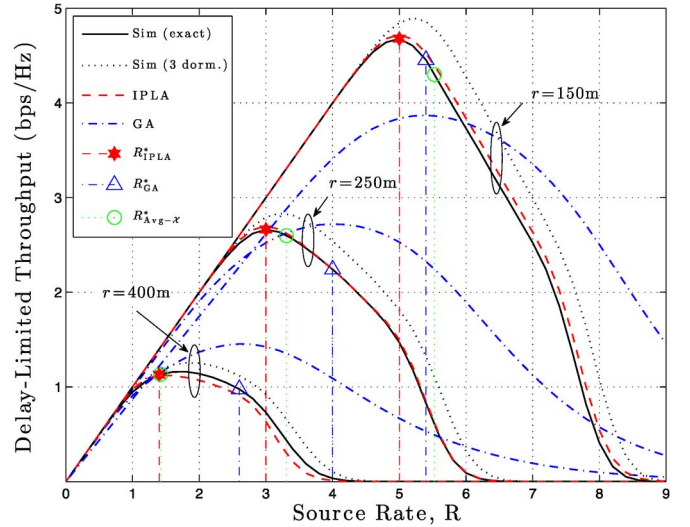


Fig. 3. Effect of user distance on RS ( $K = 6$ ,  $\theta = \pi/2$ ,  $\alpha = 3$ ,  $|w_{u_0}^{(0)}|^2 = 1$ , and  $N_{\max} = 4$ ).

conventional link adaptation schemes, i.e., GA and average interference schemes, exhibit significant differences from the actual optimal value on the exact simulation curves. The gap between the optimal source rate by the proposed IPLA and the one by the conventional GA increases as the user distance increases (i.e., as ICI increases), whereas the gap between the optimal source rate by the proposed IPLA and the one by the conventional average interference scheme increases as the user distance decreases. Therefore, we can conclude that the conventional GA is relatively good for near-BS users, while



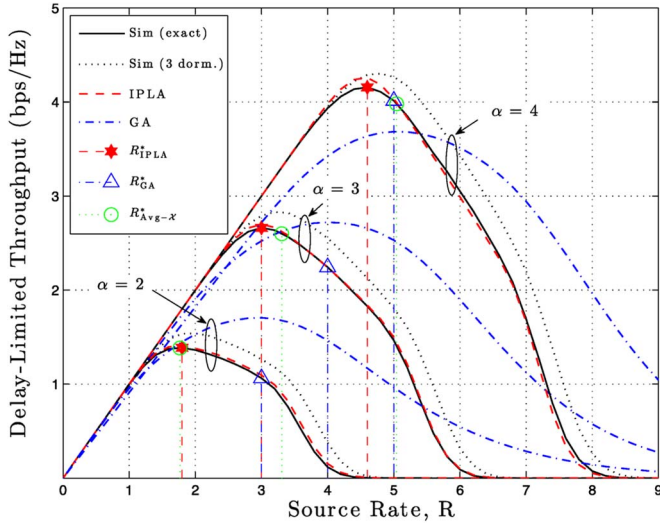


Fig. 4. Effect of path-loss exponent on rate adaptation ( $K = 6$ ,  $r = 250$  m,  $\theta = \pi/2$ ,  $|w_{u0}^{(0)}|^2 = 1$ , and  $N_{\max} = 4$ ).

the conventional average interference scheme is good for edge users, in the link adaptation perspective.

Fig. 4 shows the DLT for varying source rate  $R$  in three different path-loss exponent values. As the path-loss exponent value increases, a higher DLT is achieved since the interference is reduced with increasing the path-loss exponent value. The optimal source rate by the proposed IPLA also agrees well with the actual optimal value on the exact simulation curve, while those by the conventional schemes show significant differences. The basic trends of the differences are similar to those in Fig. 3. Consequently, for the conventional GA, the more interference exists, the larger difference occurs in the optimal source rate, while for the conventional average interference scheme, the less interference exists, the larger difference occurs in the optimal source rate. Fundamentally, both the conventional schemes exhibit significant differences with respect to the optimal source rate for large SINR values (i.e.,  $\alpha = 4$ ), which correspond to the weak interference situation. However, in a scheduling-based MU system, a user with a large SINR value has more opportunities to be selected as the best user. Therefore, it is expected that the proposed IPLA-based cross-layer policy can obtain a significant throughput gain in the viewpoint of both link adaptation and user scheduling, as compared to the conventional policies.

### C. System-Level Performance Evaluation: Cell Throughput and Fairness

Fig. 5 shows the system performance of various cross-layer policies for varying the number of users in the home cell. Specifically, Fig. 5(a) shows the system throughput of the proposed, conventional, and reference policies. The genie-aided policy  $\mathcal{P}\{\text{RS-Opt}, R_{\text{Opt}}^*\}$  provides an upper bound of the system throughput, even if it is unrealistic. The instantaneous SINR policy  $\mathcal{P}\{\text{RS-i-SINR}, R_{i\text{-SINR}}^*\}$  achieves the worst system throughput, due to rather inaccurate estimation of the ICI term caused by the channel feedback delay. The proposed IPLA-based policy  $\mathcal{P}\{\text{RS-IPLA}, S_{\text{IPLA}}(R_{\text{IPLA}}^*)\}$  always out-

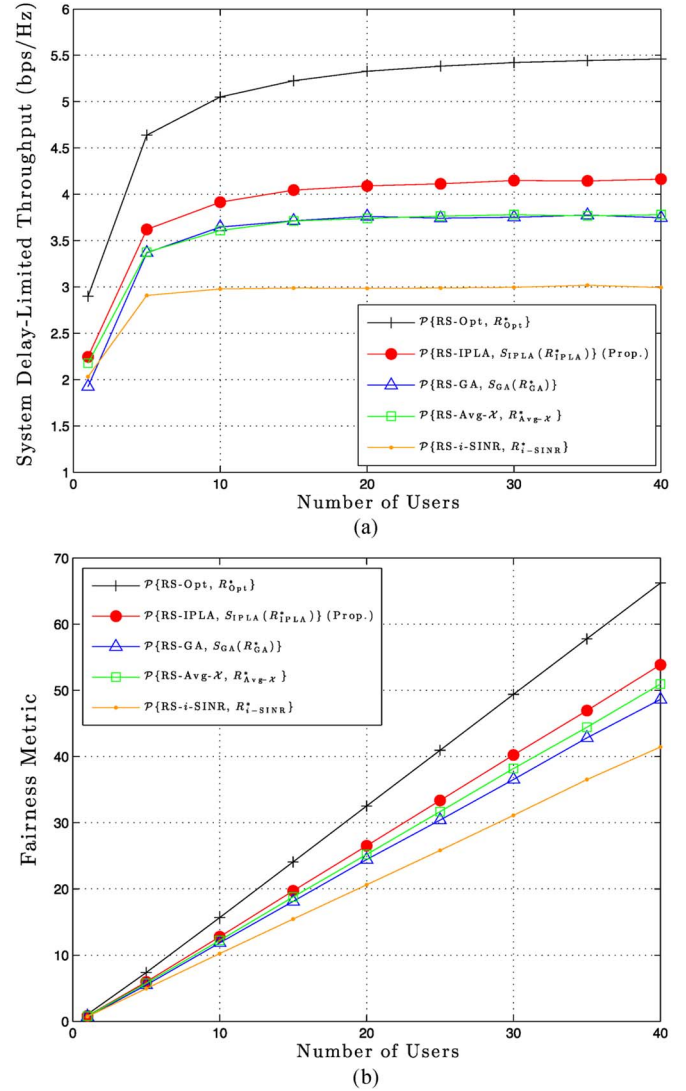


Fig. 5. System performance in an asymmetric user distribution scenario. (a) System DLT versus number of users; (b) fairness metric versus number of users ( $K = 6$ ,  $r \in [150, 200, 250, 300, 400]$  m,  $\theta = \text{Uniform}[-\pi, \pi]$ ,  $\alpha = 3$ , and  $N_{\max} = 4$ ).

performs the conventional policies  $\mathcal{P}\{\text{RS-GA}, S_{\text{GA}}(R_{\text{GA}}^*)\}$  and  $\mathcal{P}\{\text{RS-Avg-X}, R_{\text{Avg-X}}^*\}$  in the entire range of the number of users, while both the GA and average interference policies achieve almost identical system throughput. Note that, although the GA-based policy exploits statistics of the ICI term, it achieves similar system throughput to that of the average interference policy, which just utilizes an average value of the ICI term. Moreover, it achieves rather smaller system throughput than that of the proposed IPLA-based policy, which also exploits equivalent average statistics of the ICI term.

Fig. 5(b) shows the fairness metric performance of various cross-layer policies for varying the number of users in the home cell. We consider the *fairness metric* in [14], [17], [31], and [44] defined as  $\mathcal{FM}(T_1, \dots, T_N) = \sum_{u=1}^N \log(T_u)$ , where  $T_u$  denotes the achieved throughput of the  $u$ th user, and  $N$  is the number of users in the system. As investigated in the previous work, the fairness metric offers a performance measure considering both system throughput and user fairness together.

Under the PF scheduling algorithm with averaging time scale  $t_c = \infty$ , the fairness metric is maximized almost surely among the class of all schedulers [31]. As shown in Fig. 5(b), the proposed IPLA-based policy  $\mathcal{P}\{\text{RS-IPLA}, S_{\text{IPLA}}(R_{\text{IPLA}}^*)\}$  also outperforms the other three policies, except for the genie-aided policy, for all the number of users. The average interference policy  $\mathcal{P}\{\text{RS-Avg-}\mathcal{X}, R_{\text{inst}}^*\}$  rather outperforms the GA-based policy  $\mathcal{P}\{\text{RS-GA}, S_{\text{GA}}(R_{\text{GA}}^*)\}$ , in terms of the fairness metric, even if the GA-based policy exploits more information for the ICI term than the average interference policy. It comes from the fact that the GA on the aggregated ICI is inaccurate when there exist some dominant ICIs, which are general in OFDM-based cellular networks, although the GA on the aggregated ICI is well approximated for a sufficiently large number of independent and identically distributed interferers. In contrast, the proposed IPLA is highly accurate in this environment. Accordingly, the proposed IPLA-based cross-layer policy is able to be the most efficient in the OFDM-based cellular networks where there exist some dominant ICIs.

## VI. CONCLUSION

In this paper, we have investigated the joint link adaptation and user scheduling in MU and multicell environments, considering HARQ techniques. Based on the proposed mathematical approximation method for the ICI signals, the optimal transmission rate selection algorithm, in terms of the expected throughput, has been proposed. As for MU environments, a novel and effective cross-layer framework combining the link adaptation and user scheduling has been also proposed. Through extensive link-/system-level simulations, it has been shown that the proposed cross-layer policy significantly outperforms the conventional policies, in terms of both cell throughput and user fairness. With consideration of both HARQ and ICI, we have tried to investigate more general and practical communication scenarios, including MU-MIMO, receiver beamforming at users with multiple receive antennas, and HARQ technique with IR, but unfortunately, they were not mathematically tractable. Therefore, we leave these issues for future work.

## REFERENCES

- [1] E. Y. Roemer and R. L. Pickholtz, "An analysis of the effectiveness of hybrid transmission schemes," *IBM J. Res. Develop.*, vol. 14, no. 4, pp. 426–433, Jul. 1970.
- [2] D. Chase, "Code combining—A maximum-likelihood decoding approach for combining an arbitrary number of noisy packets," *IEEE Trans. Commun.*, vol. 33, no. 5, pp. 385–393, May 1985.
- [3] Y.-M. Wang and S. Lin, "A modified selective-repeat type-II hybrid ARQ system and its performance analysis," *IEEE Trans. Commun.*, vol. COM-31, no. 5, pp. 593–608, May 1983.
- [4] A. J. Goldsmith and S. G. Chua, "Adaptive coded modulation for fading channels," *IEEE Trans. Commun.*, vol. 46, no. 5, pp. 595–602, May 1998.
- [5] K. Balachandran, S. R. Kadaba, and S. Nanda, "Channel quality estimation and rate adaptation for cellular mobile radio," *IEEE J. Sel. Areas Commun.*, vol. 17, no. 7, pp. 1244–1256, Jul. 1999.
- [6] A. Goldsmith, *Wireless Communications*. Cambridge, U.K.: Cambridge Univ. Press, 2005.
- [7] D. Tse and P. Viswanath, *Fundamentals of Wireless Communication*. Cambridge, U.K.: Cambridge Univ. Press, 2005.
- [8] D. Kim, B. C. Jung, H. Lee, D. K. Sung, and H. Yoon, "Optimal modulation and coding scheme selection in cellular networks with hybrid-ARQ error control," *IEEE Trans. Wireless Commun.*, vol. 7, no. 12, pp. 5195–5201, Dec. 2008.
- [9] R. Narasimhan, "Throughput-delay performance of half-duplex hybrid-ARQ relay channels," in *Proc. IEEE ICC*, May 2008, pp. 986–990.
- [10] P. Wu and N. Jindal, "Performance of hybrid-ARQ in block-fading channels: A fixed outage probability analysis," *IEEE Trans. Commun.*, vol. 58, no. 4, pp. 1129–1141, Apr. 2010.
- [11] S. M. Kim, W. Choi, T. W. Ban, and D. K. Sung, "Optimal rate adaptation for hybrid ARQ in time-correlated Rayleigh fading channels," *IEEE Trans. Wireless Commun.*, vol. 10, no. 3, pp. 968–979, Mar. 2011.
- [12] S. M. Kim, H. Jin, W. Choi, and D. K. Sung, "Resource minimization of hybrid ARQ system with real-time traffic in time-correlated fading channels," in *Proc. IEEE ICC*, Jun. 2011, pp. 1–6.
- [13] J. Huang, R. A. Berry, and M. L. Honig, "Wireless scheduling with hybrid ARQ," *IEEE Trans. Wireless Commun.*, vol. 4, no. 6, pp. 2801–2810, Nov. 2005.
- [14] H. Zheng and H. Viswanathan, "Optimizing the ARQ performance in downlink packet data systems with scheduling," *IEEE Trans. Wireless Commun.*, vol. 4, no. 2, pp. 495–506, Mar. 2005.
- [15] W. Rui and V. K. N. Lau, "Combined cross-layer design and HARQ for multiuser systems with outdated channel state information at transmitter (CSIT) in slow fading channels," *IEEE Trans. Wireless Commun.*, vol. 7, no. 7, pp. 2771–2777, Jul. 2008.
- [16] S. M. Kim, B. C. Jung, W. Choi, and D. K. Sung, "Joint rate adaptation and user scheduling in HARQ-based multi-user systems with heterogeneous mobility," in *Proc. IEEE ISIT*, Oct. 2012, pp. 405–410.
- [17] S. M. Kim, B. C. Jung, W. Choi, and D. K. Sung, "Effects of heterogeneous mobility on rate adaptation and user scheduling in cellular networks with HARQ," *IEEE Trans. Veh. Technol.*, vol. 62, no. 6, pp. 2735–2748, Jul. 2013.
- [18] "3GPP TSG RAN; Physical channels and mapping of transport channels onto physical channels (FDD) (Release 11)," Third-Generation Partnership Project, Sophia Antipolis Cedex, France, 3GPP TS 25.211, v11.1.0, Sep. 2012.
- [19] "3GPP TSG RAN; Spreading and modulation (FDD) (Release 11)," Third-Generation Partnership Project, Sophia Antipolis Cedex, France, 3GPP TS 25.213, V11.3.0, Sep. 2012.
- [20] "E-UTRA; LTE physical layer-general description (Release 8)," Third-Generation Partnership Project, Sophia Antipolis Cedex, France, 3GPP TS 36.201, V8.3.0, Mar. 2009.
- [21] C. Kosta, B. Hunt, A. U. Qaddus, and R. Tafazolli, "On interference avoidance through inter-cell interference coordination (ICIC) based on OFDMA mobile systems," *IEEE Commun. Surveys Tuts.*, vol. 15, no. 3, pp. 973–995, Sep. 2013.
- [22] A. Damnjanovic *et al.*, "A survey on 3GPP heterogeneous networks," *IEEE Wireless Commun. Mag.*, vol. 18, no. 3, pp. 10–21, Jun. 2011.
- [23] R. Narasimhan, "Hybrid-ARQ interference channels with receiver cooperation," in *Proc. IEEE ICC*, May 2010, pp. 1–5.
- [24] S. Z. Denic, "Robust incremental redundancy hybrid ARQ coding for channels with unknown interference," in *Proc. IEEE ISIT*, Jul. 2011, pp. 1658–1662.
- [25] R.-T. Juang, K.-Y. Lin, P. Ting, H.-P. Lin, and D.-B. Lin, "Enhanced chase combining HARQ with ICI and IAI mitigation for MIMO-OFDM systems," *IEEE Trans. Veh. Technol.*, vol. 58, no. 8, pp. 4645–4649, Oct. 2009.
- [26] T. Ait-Idir, H. Chafnaji, and S. Saoudi, "Turbo packet combining for broadband space-time BICM hybrid-ARQ systems with co-channel interference," *IEEE Trans. Wireless Commun.*, vol. 9, no. 5, pp. 1686–1697, May 2010.
- [27] K. Park, D.-K. Hwang, and K.-C. Whang, "Scheduling algorithm considering HARQ and successive interference cancellation," in *Proc. IEEE Int. Conf. WiCom*, Sep. 2011, pp. 2877–2880.
- [28] A. Rácz, N. Reider, and G. Fodor, "On the impact of inter-cell interference in LTE," in *Proc. IEEE GLOBECOM*, Nov. 2008, pp. 1–6.
- [29] B. Makki, T. Svensson, T. Eriksson, and M.-S. Alouini, "Coordinated hybrid automatic repeat request," *IEEE Commun. Lett.*, vol. 18, no. 11, pp. 1975–1978, Nov. 2014.
- [30] H. Shirani-Mehr, H. Papadopoulos, S. A. Ramprasad, and G. Caire, "Joint scheduling and hybrid-ARQ for MU-MIMO downlink in the presence of inter-cell interference," *IEEE Trans. Commun.*, vol. 59, no. 2, pp. 578–589, Feb. 2010.
- [31] P. Viswanath, D. Tse, and R. Laroia, "Opportunistic beamforming using dumb antennas," *IEEE Trans. Inf. Theory*, vol. 48, no. 48, pp. 1277–1294, Jun. 2002.
- [32] M. Sharif and B. Hassibi, "On the capacity of MIMO broadcast channels with partial side information," *IEEE Trans. Inf. Theory*, vol. 51, no. 2, pp. 506–522, Feb. 2005.
- [33] "EUTRAN; Stage 2 functional specification of User Equipment (UE) positioning in E-UTRAN (Release 9)," Third-Generation Partnership Project, Sophia Antipolis Cedex, France, 3GPP TS 36.305, V9.10.0, Dec. 2012.

- [34] R. Narasimhan, "Delay-limited throughput of cooperative multiple access channels with hybrid-ARQ," in *Proc. IEEE ISIT*, Jul. 2008, pp. 409–413.
- [35] "High speed downlink packet access; Overall UTRAN description (Release 5)," Third-Generation Partnership Project, Sophia Antipolis Cedex, France, 3GPP TR 25.855, V5.0.0, Sep. 2001.
- [36] *Air Interface for Broadband Wireless Access Systems*, IEEE Std. P802.16Rev2/D1, Oct. 2007.
- [37] J. Gil-Pelaez, "Note on the inversion theorem," *Biometrika*, vol. 38, no. 3–4, pp. 481–482, Dec. 1951.
- [38] W. Choi and J. G. Andrews, "Downlink performance and capacity of distributed antenna systems in a multicell environment," *IEEE Trans. Wireless Commun.*, vol. 6, no. 1, pp. 69–73, Jan. 2007.
- [39] H. Zhu, "Performance comparison between distributed antenna and microcellular systems," *IEEE J. Select. Areas Commun.*, vol. 29, no. 6, pp. 1151–1163, Jun. 2011.
- [40] V. Witkovsky, "Computing the distribution of a linear combination of inverted gamma variables," *Kybernetika*, vol. 37, no. 1, pp. 79–90, 2001.
- [41] A. M. Mathai, "Storage capacity of a dam with gamma type inputs," *Ann. Inst. Statist. Math.*, vol. 34, no. 1, pp. 591–597, 1982.
- [42] P. G. Moschopoulos and W. B. Canada, "The distribution function of a linear combination of chi-squares," *Comput. Maths. Appl.*, vol. 10, no. 4/5, pp. 383–386, 1984.
- [43] J. D. Gibbons and S. Chakraborti, *Nonparametric Statistical Inference*, 4th ed. Boca Raton, FL, USA: CRC, 2003.
- [44] D. Tse, "Forward link multiuser diversity through rate adaptation and scheduling," presented at the Bell Labs Presentation, Holmdel, NJ, USA, Aug. 1999.

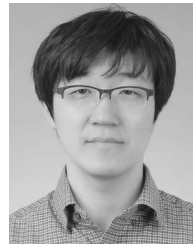


**Su Min Kim** (S'05–M'13) received the B.S. degree in electronics engineering from Inha University, Incheon, Korea, in 2005 and the M.S. and Ph.D. degrees in electrical engineering and computer science from the Korea Advanced Institute of Science and Technology (KAIST), Daejeon, Korea, in 2007 and 2012, respectively.

Since March 2015, he has been with the Department of Electronics Engineering, Korea Polytechnic University, Siheung, Korea, where he is currently an Assistant Professor. He was a Postdoctoral Researcher with the Department of Electrical Engineering, KAIST, Daejeon, Korea, from February to August 2012; with the Department of Information and Communication Engineering, Gyeongsang National University, Tongyeong, Korea, from September to October 2012; and with the School of Electrical Engineering, KTH Royal Institute of Technology, Stockholm, Sweden, from November 2012 to November 2014. From November 2014 to February 2015, he was an Experienced Researcher in Radio Access Technology with Ericsson Research, Stockholm, Sweden. His research interests include next-generation mobile communication systems, hybrid automatic repeat request (HARQ) protocols, radio resource management, interference management, cooperative and buffer-aided relaying communications, cognitive radio communications, machine-type communications, and statistical signal processing.

Dr. Kim received the Paper Award from the Next Generation PC International Conference in 2005; the Silver and Bronze Awards from the 17th and 18th Samsung Humantech Thesis Prizes in 2011 and 2012, respectively; and the Travel Grant for the IEEE International Conference on Communications from the Ericsson Research Foundation in 2013.

Dr. Kim received the Paper Award from the Next Generation PC International Conference in 2005; the Silver and Bronze Awards from the 17th and 18th Samsung Humantech Thesis Prizes in 2011 and 2012, respectively; and the Travel Grant for the IEEE International Conference on Communications from the Ericsson Research Foundation in 2013.



**Bang Chul Jung** (S'02–M'08–SM'14) received the B.S. degree in electronics engineering from Ajou University, Suwon, Korea, in 2002 and the M.S. and Ph.D. degrees in electrical and computer engineering from the Korea Advanced Institute of Science and Technology (KAIST), Daejeon, Korea, in 2004 and 2008, respectively.

From January 2009 to February 2010, he was a Senior Researcher/Research Professor with the KAIST Institute for Information Technology Convergence. From March 2010 to August 2015, he was a Faculty of Gyeongsang National University, Tongyeong, Korea. He is currently an Associate Professor of the Department of Electronics Engineering, Chungnam National University, Daejeon, Korea. His research interests include cellular networks, Fifth-Generation mobile communication systems, compressed sensing, interference management, multiple-input–multiple-output (MIMO) and multiple-access techniques, random access, and radio resource management.

Dr. Jung received the Fifth IEEE Communication Society Asia-Pacific Outstanding Young Researcher Award in 2011. He also received the Bronze Prize of Intel Student Paper Contest in 2005, the First Prize at KAIST's Invention Idea Contest in 2008, the Bronze Prize at the Samsung Humantech Paper Contest in 2009, the Outstanding Research Award from the Institute of Marine Industry at Gyeongsang National University in 2013, and the Gaechuck Award for Excellence in Teaching of Gyeongsang National University in 2014.



**Dan Keun Sung** (S'80–M'86–SM'00–F'15) received the B.S. degree in electronics engineering from Seoul National University, Seoul, Korea, in 1975 and the M.S. and Ph.D. degrees in electrical and computer engineering from The University of Texas at Austin, Austin, TX, USA, in 1982 and 1986, respectively.

Since 1986, he has been with the faculty of the Korea Advanced Institute of Science and Technology (KAIST), Daejeon, Korea, where he is currently a Professor with the Department of Electrical Engineering. From 1996 to 1999, he was the Director of the Satellite Technology Research Center (SaTReC), KAIST. His research interests include mobile communication systems and networks, with special interest in resource management, smart grid communication networks, machine-to-machine communications, wireless local area networks, wireless personal area networks, traffic control in wireless and wired networks, performance and reliability of communication systems, and microsatellites.

Dr. Sung is a member of the National Academy of Engineering of Korea. He received the 1992 National Order of Merits; the Dongbaek Medal for successfully developing, launching, and operating the first Korean satellite in history; the 1997 Research Achievement Award; the 1997 IEEE International Workshop Mobile Multimedia Communications (MoMuC) Paper Award, the 2000 Academic Excellence Award; the Best Paper Award from the Asia-Pacific Conference on Communications in 2000; the Scientist of the Month from the Ministry of Science and Technology and the Korea Science and Engineering Foundation in 2004; the Patent Award for Top 10 Most Patent Registrations among professors in all fields (and the first in the field of electrical engineering) from the Korean Intellectual Property Office; and the 2013 Haedong Academic Grand Award from the Korean Institute of Communications and Information Sciences. He had served as a Division Editor of the *Journal of Communications and Networks* from 1998 to 2007. He also had served as the Editor of the IEEE COMMUNICATIONS MAGAZINE from 2002 to 2011.